Water Flow Velocity Driven Modified Savonius Hydrokinetic Turbine

Thochi Seb Rengma and P. M. V. Subbarao
Indian Institute of Technology Delhi, India
Email: Thochi.Seb.Rengma@mech.iitd.ac.in, pmvs@mech.iitd.ac.in

Abstract*—Hydrokinetic turbines are new technologies to harness the kinetic energy of river streams without impounding the concreate structure across the natural flow of water. These turbines can provide an alternative solution to generate the clean and sustainable energy from rivers, natural water streams, and tidal or marine currents where the water flow velocity is relatively uniform and one directional. This turbine can also be installed as a standalone off-grid power generation for domestic houses, especially for the houses in villages, which is located far from the main grid. This study is aimed to quantify the high dynamic interaction and complexity of the turbine blades and the turbulent flow to optimize the power coefficient and to study the critical prerequisites for utilizing the full potential. Such hydrokinetic turbine is still in the research phase and yet to be commercially installed in India. Savonius hydrokinetic turbine (SHKT) is the simplest of all hydrokinetic turbine. It can be easily construct and repair by local inhabitants and can be even easily dispose to the environment. In this study, CFD analysis is performed on a SHKT with circular blades, 90 °helical blades, 180 °helical blades and modified Savonius hydrokinetic turbine by varying the blade arc-angle and blade shape factor to analyse the parameters influencing the power coefficient. Unsteady Reynolds Average Navier-Stokes equation (URANS) solver has been applied for numerical analysis with realizable k-ε (Enhance wall Fn.) turbulence model. The study compared to the circular turbine shows that 180 °helical, modified SHKT and 90 °helical SHKT results in an increase of 6.5%, 16.1%, 33.6% in power coefficient.

***Index Terms*— Savonius hydrokinetic turbine, helical blades, blade arc-angle, blade shape-factor**

Nomenclature	
H	Height of turbine [m]
D	Diameter of turbine [m]
D_o	Diameter of end plate [m]
p	Straight edge of the plate [m]
q	Radius of the circular arc [m]
e	Gap between the two blades [m]
t	Thickness of the blades [m]
ω	Angular velocity [rad/s]
ρ	Density of water [kg/m^3]
Φ	Blade arc-angle [degree]
P	Power [W]
Cp	Power coefficient
Cm	Moment coefficient
Abbreviations	
A	Area (H*D) [m^2]
U	Free stream velocity [m/s]
g	Gravitational acceleration [m/s^2]
AR	Aspect ratio [H/D]
OR	Overlap ratio [e/D]
TSR	Tip speed ratio [ωD/2U]

I. Introduction

Based on REN21's 2020 report [1], renewable energy contributed for almost 21% of total final energy consumption worldwide. In 2017, an estimated 19 GW of new hydropower capacity was added globally, increasing the total capacity to around 1,114 GW. In general, there are two types of hydrokinetic turbines: The horizontal axis and the vertical axis [2], [3]. Horizonal axis turbine have better efficiency compared to the vertical axis turbine. But vertical axis turbine is the simplest to construct and cost effective [4]. Vertical axis wind turbines have piqued the interest of researchers over the years, resulting in enough developments in the technology to make it a viable energy harvester in a variety of wind environments. However, in the recent decade, research into this technique for gathering river streams has increased. The Savonius turbine that has piqued the curiosity of scientists in recent years [5].

In the year 1920, S. J. Savonius developed the Savonius turbine [6]. The working principle of the river hydrokinetic turbine system are shown in Fig. 1. The turbine shape resembles the letter S, by combination of two semicircular

doi: 10.18178/ijmerr.11.5.296-303

blades. [7]. A geometric parameter of SHKT are shown in Fig. 2.

The turbine rotates because of the difference in drag between the both the turbine blades. The net driving force can be enhanced by increasing the positive force on the advancing blade or by reducing the forces on the returning blade [8]. Because the river only flows in one direction, the rotor rotates around its axis, causing a change in coefficient of drag on both the advancing and returning blades, resulting in a change in torque generated by a rotor at constant ω . During the rotation of the rotor, the change in torque fluctuates cyclically. [9]. Hydrokinetic turbines convert the kinetic energy of flowing river into mechanical power. Hydrokinetic turbines are also called ultra-low head hydro turbines and zero head water turbines [10]. These turbines offer many advantages like simple construction, low noise, reduced wear on moving parts, better self-starting, etc. [11].

Saha *et al.* [12] goal of was to see if a twisted bladed Savonius rotor could be used to generate electricity. According to the study, as twist angles increase, energy collection in the bottom half of the blade decreases progressively compared to the top part, resulting in a decrease in net positive torque. At a TSR of 0.65, a twisted blade with a 15^{o} angle has a maximum Cp of 0.131.

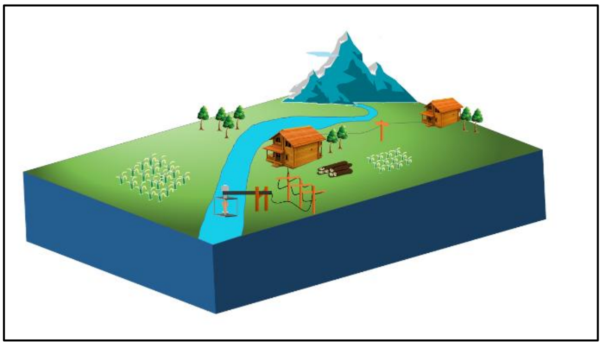

Figure 1. The working principle of the SHKT system

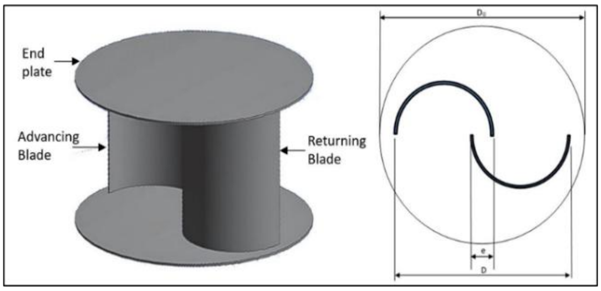

Figure 2. Geometrical parameters of SHKT

Kamoji *et al.* [13] conducted experiments on helical Savonius blades. Each helical Savonius rotor had its torque and power coefficients tested. At different overlap ratios, such as 0.0, 0.1, and 0.16, the performance of helical rotors with and without shaft between the end plates was studied, and it was discovered that the helical Savonius rotor with shaft had the lowest coefficient of power of 0.09 at a TSR of 0.9.

Kamoji *et al*. [14] conducted test in an open flow wind tunnel. They studied the rotor with and without a shaft in between the blades, comparing the results to the traditional Savonius rotor. The results showed that at Reynolds number 1,50,000, a modified Savonius rotor (without shaft) with an overlap ratio of 0.0, blade shape factor (p/q) of 0.2, blade arc-angle of 124°, and an aspect ratio of 0.7 provides maximum Cp of 0.21, whereas a circular Savonius blade and a modified Savonius blade (with shaft) provide Cp of 0.175 and 0.143, respectively.

Roy and Saha [15] after researching a range of blade designs, they produced a novel blade profile. The results demonstrate that the novel blade profile outperformed modified Bach, Benesh, semi-elliptical, and standard SSWTs by 3.3 percent, 6.9 percent, 19.2 percent, and 34.8 percent, respectively. The maximum torque coefficient of newly designed blades has increased by 31.6 percent. With wind tunnel obstruction correction, the newly designed SSWT achieved a maximum power coefficient of 0.31.

Wahyudi *et al.* [16] studied on increasing the swept area of the Savonius Tandem Blade. For variation in Tandem Blade Savonius (TBS), such as Overlap, Symmetry, and Convergence, the investigation was done at a water velocity of 1 m/s. In the investigation, it was discovered that at a rotor angle of 90°, an advancing blade begins to develop in order to provide ideal drag force. The maximal performance of convergence TBS is reached when the rotor angle approaches 150°. According to the findings, the convergence type TBS has the best performance, allowing for a greater pressure gap between upstream and downstream.

Tartuferi *et al.* [17] presented two novel airfoil blade forms, dubbed SR3345 and SR5050, to increase the performance of Savonius rotors by raising the mean Camber line of an existing base airfoil shape. According to the study, a low-pressure zone which is formed at advancing blade, can lead to better blade rotation and hence increased power production.

Different researchers have studied on various turbine blade shape and blade angles. But their study does not include the comparison of performance analysis of turbine for the same blade swept area. This study would provide the optimal blade of SHKT, for same swept area, for producing power at a competitive rate for residential and commercial applications when the channel width is fixed. In the present study, the turbine aspect ratio of 1.8 is considered, which gives a better performance [18]. The overlap ratio of 0.16 was decided for the SHKT, in which the proper overlap ratio was found between 0.15 to 0.25 [18]. The present computational analysis does not include shaft in between the end plates as it provides better performance [14].

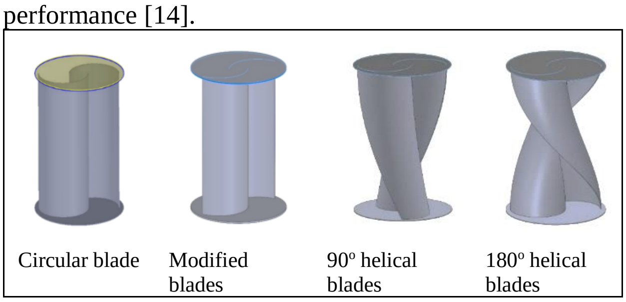

Figure 3. Models of different hydrokinetic blades

The objective of the present study is to compare the performance of circular, modified blades, 90 º helical and 180º helical blades for the same swept area. In the present investigation, different blade arc-angle and shape factor have been investigated for modified blade. The following sections include parametric blade design and performance, computational modelling, validation, grid independent test, results and discussion followed by conclusions.

The study was carried out in CFD, Ansys Fluent 19.1 software for computational analysis. The investigation was carried out to improve the geometry of a SHKT for higher torque to produces higher power coefficient. The turbines that were investigated in this present study are shown in Fig. 3. The current study includes:

i. The performance analysis of circular blades and validating the present computational results with the published experimental data.
ii. The parametric analysis of the blade arc-angle (Φ) and the blade shape factor (p/q) for Tip Speed Ratio varying from 0.4 to 1.1. Table 1 shows the geometrical parameters considered for the numerical simulations.
iii. Comparison of the performance of 90º and 180º helical blades of SHKT.

As the results will indicate, the substantial improvements in the power coefficient make SHKT an alternative for producing power for small residential in villages and commercial applications.

II. Design and Performance Parameter

Savonius hydrokinetic theoretical power can be calculated as [19]:

$$P_{Theory/in} = \frac{1}{2}\rho AU^3 = \frac{1}{2}\rho HDU^3 \tag{1}$$

Because of the blades' profile, the whole energy that goes through the blades does not account to the turbine's spinning. As a result, the turbine cross-section can only catch a fraction of the Kinetic Energy (KE), also known as the power coefficient (Cp). The turbine's actual power output is reported as:

$$P_{Turbine} = C_P \frac{1}{2}\rho AU^3 \tag{2}$$

The tip-speed ratio is defined as the speed of the blade at the tip to the speed of flowing water, determines the power coefficient of hydrokinetic turbines [20]. It can be expressed as:

$$\lambda = \frac{speed\ of\ blade\ at\ tip}{speed\ of\ flowing\ water} = \frac{\omega D}{2U} \tag{3}$$

The expression for outlet power extraction (P_{out}) is given as:

$$P_{out} = T\omega = \frac{2\pi NT}{60} \tag{4}$$

The torque coefficient (C_m) is generally expressed as:

$$C_m = \frac{T}{\frac{1}{2}\rho AU^2 R} = \frac{2T}{\frac{1}{2}\rho HD^2 U^2} \tag{5}$$

The power coefficient (Cp) is defined as the ratio of power input to power output. The expression is given as:

$$C_p = \frac{P_{out}}{P_{in}} = \frac{T\omega}{\frac{1}{2}\rho HDU^3} = C_m\lambda \tag{6}$$

The maximum efficiency of an ideal turbine for a uniform flow condition is equal to Cp max= 0.593, which is also know at the Betz limit.

TABLE I. Parameter Investigated for Numerical Analysis

Blade arc-angle (Φ)	Blade shape factor (p/q)
115 º, 124 º, 140 º, 160 º	0, 0.2, 0.4, 0.6

III. Computational Modeling

A. Computational Domain

Ansys Design Modeler was used to create 3D geometry based on the parameters listed in Table II. To collect the angular velocity of the turbine, a cylinder casing was built around it. To compute the turbine's rotation, the computational domain is separated into two zones (outer stationary zone and inner rotating zone). To preserve flow continuity, the cylinder's circumference was configured as an interface. The three dimensional channel domain is shown in Fig. 4.

B. Mesh Generation

TABLE II. Mesh Details

Quality aspect	Circular blades	Modified blade	Helical 90 º	Helical 180 º
Elements	8203238	8877043	8689731	6680157
Nodes	1881669	1966512	2530567	1445466

As illustrated in Fig. 5, a non-conformal unstructured grid with tetrahedral components was employed for meshing. To capture the flow behavior near the turbine blades, an inflating layer was produced near them. The quality of the mesh created is seen in Table II.

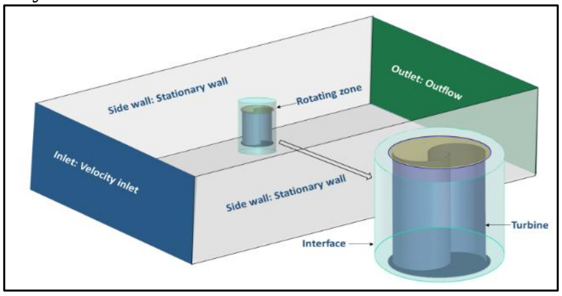

Figure 1. 3D computational domain

C. Boundary Condition and Solver Simulation

Table III lists the boundary conditions that were employed in the numerical analysis. The velocity intake (Dirichlet boundary condition) was chosen as the inlet boundary condition, which corresponds to free steam velocity. Outflow is specified as the outlet boundary condition. Symmetry was allocated to the channel's top. Wall borders were established on the sides and bottom.

TABLE III. PARAMETER CONSIDERED FOR GRID INDEPENDENT TEST

Parameter Investigated	value
No. of blades	2
Overlap ratio (e)	0.2
Blade diameter (D), m	0.33
Blade height (H), m	0.23
Endplate diameter (D_0), m	0.363
Blade thickness (m)	0.002
Shaft diameter, a (m)	0.015

The steady-state solver with MRF is used to specify the domain rotation, and the solution is then simulated in a transient manner using a sliding mesh motion approach. The MRF simulation's convergent steady state result is utilised to initialise the transient SMM solver. To solve the transient flow problem, a Finite Volume Method (FVM) Multiple Reference Frame (MRF) was applied to a revolving zone and set at an angular velocity. To discretize convective terms, a second order Upwind approach was used, and the pressure was interpolated using a linear interpolation scheme.

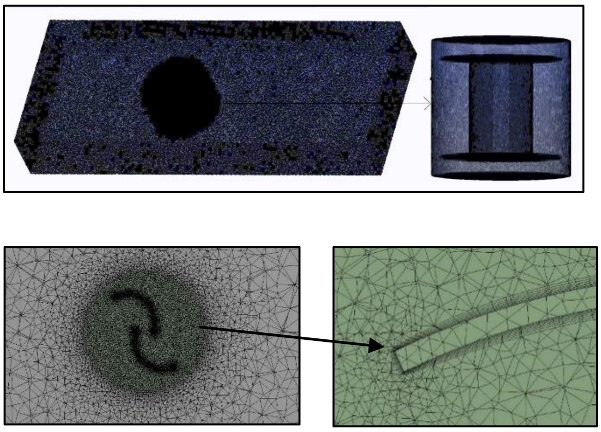

Figure 5. Meshing of the modified blade in model channel

A central difference scheme was used to solve the diffusive terms. Semi-Implicit Methods for Pressure-Linked Equations were used to solve the pressure velocity coupling (SIMPLE). For each time step, convergence criteria were obtained at a residual value of 10^{-5}. Moment coefficients (Cm) were simulated over time with correct reference values in the case of the transient solver. For each case, the value of time step size is determined by the value of RPM. For every 5 degrees of model rotation, time steps are calculated. 350 time steps each simulation are conducted for 6 complete rotations, with 40 iterations every time step.

D. Turbulence Model

The selection of the turbulence model is selected based on the comparing the computational results with the experimental results. In this study, Realizable k-ε model has been selected since it shows minimum error when compared with the experimental data. Also is known for better simulation capturing the behavior of the blades curvature. [21]. This model comprises of turbulent viscosity and a new transport equation for the dissipation rate ε. The turbulence model is validated with the published experimental results.

IV. RESULTS AND DISCUSSION

The details results are discussed below:

i. Firstly, grid independency test is conducted to capture the accurate value of performance and to reduce the computational time.

ii. The input boundary conditions for the computational analysis are collected from the published experimental result to validate the present results with the published result. The parameter considered for the grid independent test are given in Table IV.

TABLE IV. BOUNDARY CONDITION OF COMPUTATIONAL SIMULATIONS

Name	Boundary conditions	Values
Inlet	Velocity inlet	1.5 m/s
Outlet	Outflow	Outflow
Top wall	Symmetry	Symmetry
Side and bottom wall	Free slip wall	Wall
Rotating zone	MRF	Rotates at desired rpm
Turbine	No slip	stationary

iii. Numerical simulations are carried out for modified blade, 90º & 180º helical blade. Power coefficient are calculated to determine the performance of each turbine. Results are discussed and compared to the circular blade.

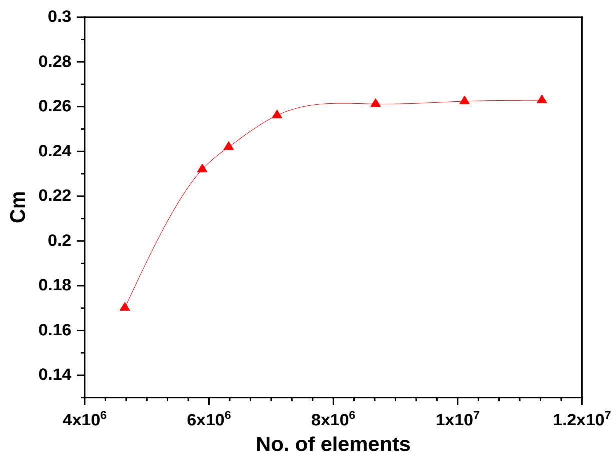

Figure 6. Moment coefficient vs number of elements

A. Grid Independent Test and Validation

The simulations are performed for different mesh elements to optimize the simulation time. The moment coefficient remains almost constant after certain elements sizes which is shown in Fig. 6. The published experimental data for input numerical simulations are shown in Table V.

TABLE V. BOUNDARY CONDITION FOR COMPUTATIONAL SIMULATIONS

Name	Boundary condition	Value
Inlet	Velocity inlet	6 m/s
Outlet	Outflow	Outflow
Top channel	Symmetry	symmetry
Channel Side and bottom wall	No slip wall	stationary
Turbine	No slip wall	stationary
Inner zone	MRF	Rotates at desired RPM

Different turbulence model are compared against varying TSR to validate the present study with the published experimental result, which is shown in Fig. 7.

Realizble k- ε model is found to have a similar trend with the experimental data. The value of the moment coeffeceint decreases with the increasing TSR. The error between the experimental and computation datas are below 10%. The comparision of moment coeffecient againt the angle of rotaion for different TSR is also shown in Fig. 8. Hence realizable k- ε (Enhance wall Fn.) model is used for analysis of the following numerical solutions.

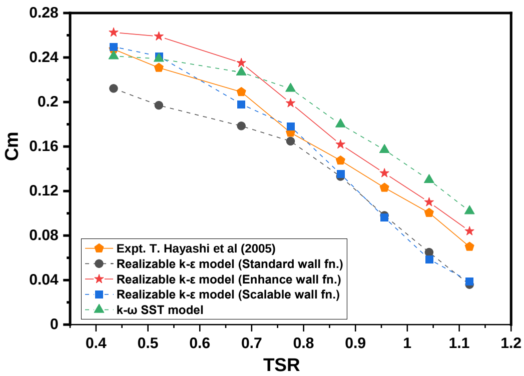

(a)

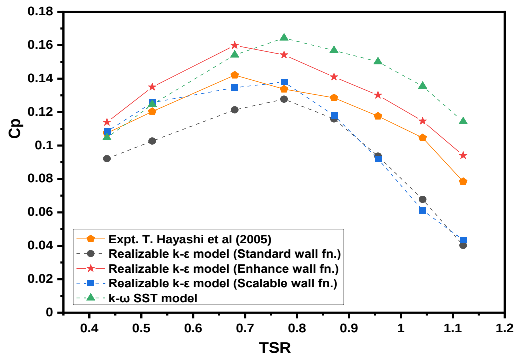

(b)

Figure 7. Validation of turbulence model (a) Moment coefficient (b) Power coefficient, with publish results

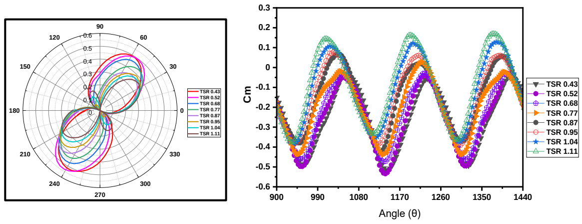

(a) (b)

Figure 8. Cm vs. angle of rotation comparison for different value of TSR (a) polar coordinates (r,θ) (b) The sinusoidal behavior

B. Parametric Analysis of Modified Blade

Parametric analysis of blade arc-angle (Φ) and the blade shape factor (p/q) on the circular blades and the modified Savonius hydrokinetic turbine are numerically analysis to optimize their performance. The top view of the modified blades is shown in Fig. 9. Table VI shows the geometric parameter of the modified SHKT. Fig. 11 represent the grid independent test, which is initially performed to optimize the optimal time and mesh element for the same geometry.

Four cases were considered during the numerical analysis of modified SHKT. The four cases include the blade arc-angle fluctuated from 115º to 160º corresponding to the blade shape factor (p/q) = 0.0, 0.2, 0.4 and 0.6. The case of p/q = 0 and Φ = 180º corresponds to circular blade.

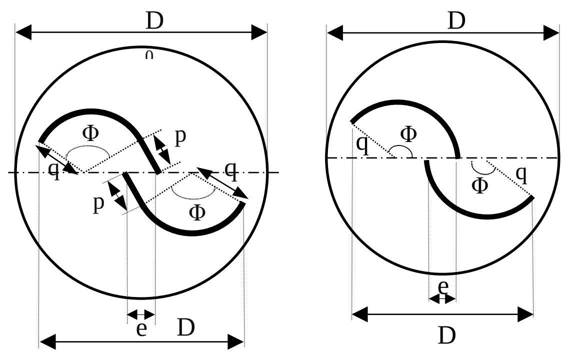

(a) Modified savonius rotor having Φ and p/q

(b) Modified blade having Φ and p/q = 0

Figure 9. Top view of modified Savonius rotor

1) measurements of torque and power coefficients

Using the performance formulae, the torque and power coefficients have been computed. For each of the four examples, the power coefficients were calculated using Equation (5). For Case 1, the greatest value of Cm reached was 0.3795 at a TSR of 0.5 for the value of 124º shown in Fig. 10 for the blade shape factor (p/q=0). At TSR levels of 0.5, case 2,3, and 4 arrangements with p/q = 0.2, 0.4, and 0.6 obtained a peak Cm of 0.376 (Φ=115º), 0.338 (Φ =140º), and 0.365 (Φ =115º).

The largest value of Cp achieved in Case 1 was 0.224 at a TSR of 0.7 at Φ=124º. In Case 2, the turbine had the greatest Cp value of 0.198 with a TSR of 0.7 for a value of Φ=140º. In Case 3, the turbine had the greatest Cp value of 0.187 at a TSR of 0.7 for a value of Φ=140º. In Case 4, the turbine had the greatest Cp value of 0.192 with a TSR of 0.6 for Φ=115º. The peak values for instances case 1, 2, and 3 corresponded to TSR 0.7, whereas the peak value for case 4 corresponded to TSR 0.6. The torque coefficient values, and therefore the torque operating on the turbine, are directly dependent on the efficiency of the turbine, as shown by the formulae used to compute the value of Cp. The design of the returning blade in Case 1 does not create a negative drag, which aids the turbine's spinning. Fig. 13 depicts the reduction of negative torque owing to the ideal form. Case 1 had a peak value of Cp of 1.4% , 16.3% , and 14% greater than Cases 2, 3, and 4, respectively. Comparing the modified blades to circular blades, case 1 and case 2 perform 3% and 16% better, respectively. As a result, it is apparent that the blade arc-angle and blade form component both contribute to a larger Cp value.

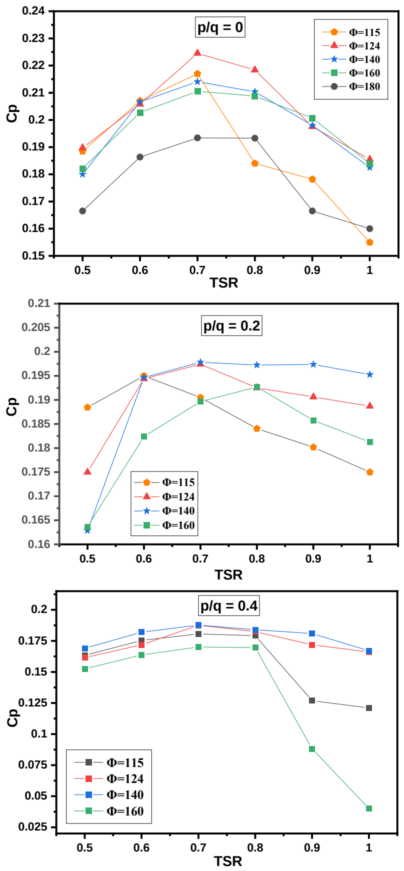

C. *Performance of 90º and 180º Helical SHKT*

TABLE VI. GEOMETRIC PARAMETER OF MODIFIED SHKT

Parameter	value
No. of turbine blades	2
Turbine aspect ratio (H/D)	1.8
Turbine overlap ratio (e)	0.2
Blade diameter (D), mm	250
Blade height (H), mm	450
Endplate diameter (D_0), mm	275
Blade arc-angle (Φ), degree	115 º, 124 º, 140 º, 160 º
Blade shape factor, (p/q)	0.0,0.2, 0.4, 0.6
Blade thickness (mm)	2

The helical SHKT have an advantages of positive moment coefficient throughout the revolution. This type of blades have certain advantages in the self-starting torque. The maximum power coefficient of 90º helical SHKT obtained is 0.2585 at TSR value of 0.7. The maximum power coefficient for the case of 180º helical SHKT is 0.20 at TSR value of 0.7.

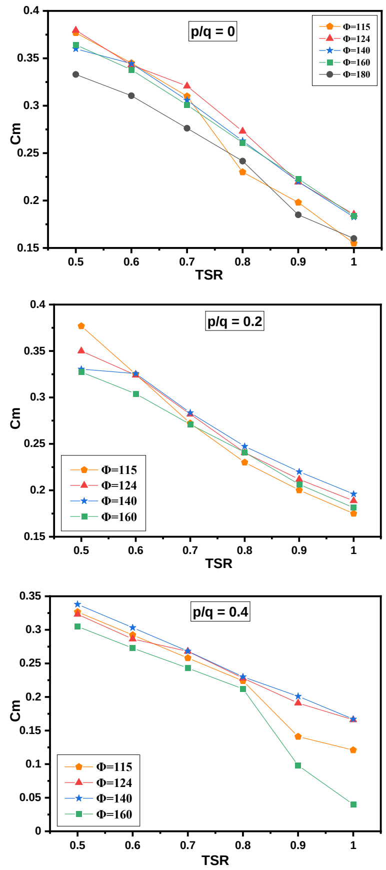

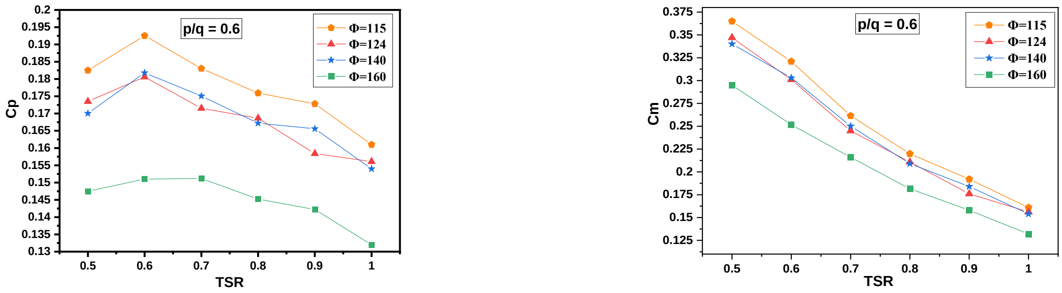

Figure 10. The value of Cp and Cm for four cases corresponding to TSR

The comparison of moment coefficient and power coefficient for both 90 º and 180 º helical SHKT for the TSR value ranging from 0.5 to 1.1 is shown in Fig. 12 and Fig. 13.

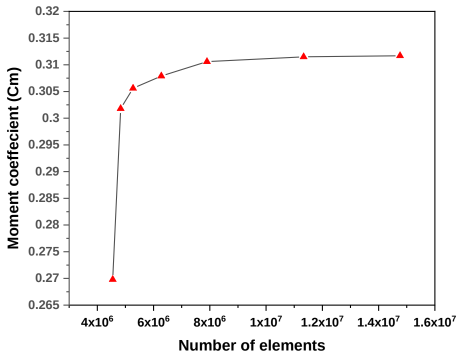

Figure 11. Moment coefficient vs number of elements

All the four blades have been computationally analysis. The modified, 90º and 180º helical SHKT shows better performance compared with the circular blades. From Fig 13, it can be concluded that the self-starting torque is found best in the case of 180 helical SHKT.

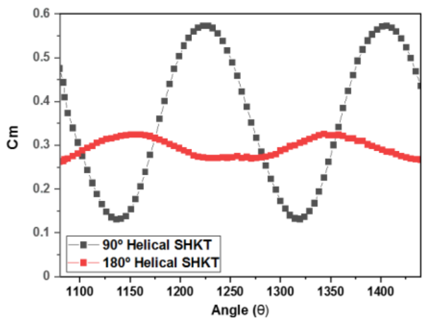

Figure 12. Cm vs. angle of rotation comparison for 90 ° and 180 ° helical SHKT

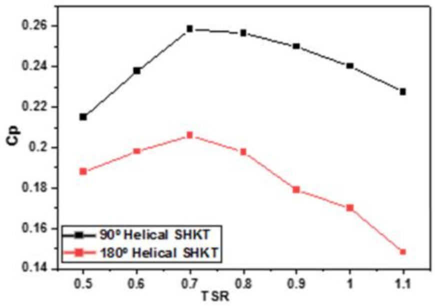

Figure 13. Cp vs TSR comparison 90 ° and 180 ° helical SHKT

This new turbine shows better performance, self-starting torque at every stage of rotation angle. The value of Cm and Cp corresponding to different value of TSR for all the four blades are shown in Fig. 14 and Fig. 15. The average static torque coefficient of all the studied turbine corresponding to TSR 0.7 are presented in Fig. 16. The maximum power coefficient achieve in the present study is 0.2585 for 90º helical SHKT obtained at TSR value of 0.7. Modified SHKT can be a good option for the arrangement having deflector blades as the value of Cm is higher than the other turbines.

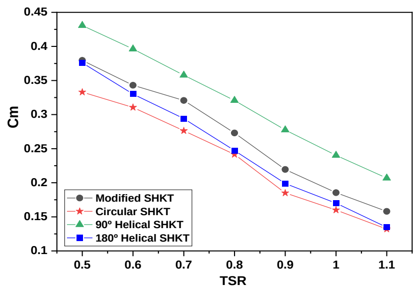

Figure 14. Cm vs TSR comparison of circular and modified Savonius turbine (p/q= 0, Φ=124)

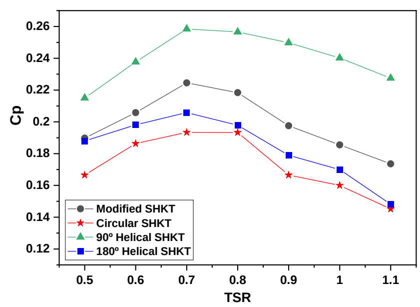

Figure 15. Cp vs TSR comparison of circular and modified Savonius turbine (p/q= 0, Φ=124)

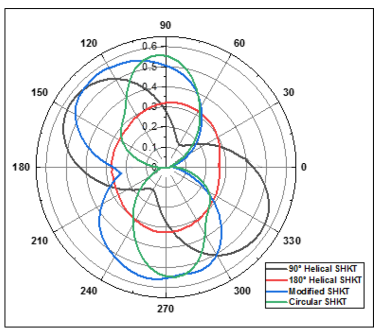

Figure 16. Average of static torque coefficients at TSR= 0.7

V. CONCLUSION

Based on the present study, the following findings have been drawn:

i. The maximum power coefficient (C_{Pmax}) of 0.258 was achieved in the case of 90 °helical SHKT at a TSR of 0.7.
ii. The helical SHKT yields better self-starting characteristics and provides positive moment coefficient throughout the turbine rotation.
iii. The modified SHKT, corresponding to Φ=124° and p/q=0 have C_{Pmax} of 0.224 at a tip speed ratio (TSR) of 0.7.
iv. The 180 ° helical SHKT, modified blade and 90 ° helical SHKT hydrokinetic turbine results in an increase of 6.5%, 16.1 % and 33.6% respectively compared to the circular SHKT.

CONFLICT OF INTEREST

The authors declare no conflict of interest.

AUTHOR CONTRIBUTIONS

Thochi Seb Rengma conducted the research; Prof. P.M.V. Subbarao analyzed and interpret the results. All authors had approved the final version.

ACKNOWLEDGMENT

The authors wish to thank his lab mates Mr. Devashri Mourya, Mr. Hariom Saran Singh and Mr. Mahendra Gupta for their guidance and HPC (IIT Delhi) team for high-speed computational assistant.

REFERENCES

[1] REN21. "Renewable Now." [Online]. Available: https://www.ren21.net/.
[2] A. De Marco, D. P. Coiro, D. Cucco, and F. Nicolosi, "A numerical study on a vertical-axis wind turbine with inclined arms," *Int. J. Aerosp. Eng.*, vol. 2014, 2014.
[3] M. K. Gupta and P. M. V. Subbarao, "Development of a semi-analytical model to select a suitable airfoil section for blades of horizontal axis hydrokinetic turbine," *Energy Reports*, vol. 6, no. February, pp. 32–37, 2020.
[4] M. B. Salleh, N. M. Kamaruddin, and Z. Mohamed-Kassim, "Savonius hydrokinetic turbines for a sustainable river-based energy extraction: A review of the technology and potential applications in Malaysia," *Sustain. Energy Technol. Assessments*, vol. 36, no. July, p. 100554, 2019.
[5] T. S. Rengma, A. R. Sengupta, M. Basumatary, A. Biswas, and D. Bhanja, "Performance analysis of a two bladed Savonius water turbine cluster for perennial river-stream application at low water speeds," *J. Brazilian Soc. Mech. Sci. Eng.*, vol. 43, no. 5, 2021.
[6] S. J. Savonius, *The Wing Rotor in Theory and Practice*, 1925.
[7] S. Savonius, "The S-rotor and its applications," *Mech. Eng.*, vol. 53, no. 5, pp. 333-338, 1931.
[8] M. A. Kamoji, S. B. Kedare, and S. V. Prabhu, "Experimental investigations on single stage, two stage and three stage conventional Savonius rotor," *Int. J. energy Res.*, vol. 32, no. 2008, pp. 877–895, 2008.
[9] T. S. Rengma and P. M. V. Subbarao. (2022). Comparative analysis of savonius type ultra-micro hydrokinetic turbine of experimental and computational investigation. p. 380, [Online]. Available: 10.1007/978-981-16-3497-0_19.
[10] M. J. Khan, G. Bhuyan, M. T. Iqbal, and J. E. Quaicoe, "Hydrokinetic energy conversion systems and assessment of horizontal and vertical axis turbines for river and tidal applications: A technology status review," *Appl. Energy*, vol. 86, no. 10, pp. 1823–1835, 2009.
[11] R. Gupta, A. Biswas, and K. K. Sharma, "Comparative study of a three-bucket Savonius rotor with a combined three-bucket Savonius-three-bladed Darrieus rotor," *Renew. Energy*, vol. 33, no. 9, pp. 1974–1981, 2008.
[12] U. K. Saha and M. J. Rajkumar, "On the performance analysis of Savonius rotor with twisted blades," *Renew. Energy*, vol. 31, no. 11, pp. 1776–1788, 2006.
[13] M. A. Kamoji, S. B. Kedare, and S. V. Prabhu, "Performance tests on helical Savonius rotors," *Renew. Energy*, vol. 34, no. 3, pp. 521–529, 2009.
[14] M. A. Kamoji, S. B. Kedare, and S. V. Prabhu, "Experimental investigations on single stage modified Savonius rotor," *Appl. Energy*, vol. 86, no. 7–8, pp. 1064–1073, 2009.
[15] U. K. Saha, S. Thotla, and D. Maity, "Optimum design configuration of Savonius rotor through wind tunnel experiments," *J. Wind Eng. Ind. Aerodyn.*, vol. 96, no. 8–9, pp. 1359–1375, 2008.
[16] B. Wahyudi, S. Soeparman, S. Wahyudi, and W. Denny, "A simulation study of flow and pressure distribution patterns in and around of Tandem Blade Rotor of Savonius (TBS) hydrokinetic turbine model," *J. Clean Energy Technol.*, vol. 1, no. 4, pp. 286–291, 2013.
[17] M. Tartuferi, V. D'Alessandro, S. Montelpare, and R. Ricci, "Enhancement of savonius wind rotor aerodynamic performance: A computational study of new blade shapes and curtain systems," *Energy*, vol. 79, no. C, pp. 371–384, 2015.
[18] V. Patel, G. Bhat, T. I. Eldho, and S. V. Prabhu, "Influence of overlap ratio and aspect ratio on the performance of Savonius hydrokinetic turbine," *Int. J. Energy Res.*, vol. 41, no. 6, pp. 829–844, 2017.
[19] L. Pham and S. Member, "Riverine hydrokinetic technology : A review," *Oregon Tech - Ree516 Term Pap.*, pp. 1–6, 2014.
[20] B. Jones, *Elements of Aerodynamics*, New York: J. Wiley, 1889.
[21] M. H. Mohamed, G. Janiga, E. Pap, and D. Thévenin, "Optimal blade shape of a modified Savonius turbine using an obstacle shielding the returning blade," *Energy Convers. Manag.*, vol. 52, no. 1, pp. 236–242, 2011.

Thochi Seb Rengma is research scholar in Mechanical Engineering Department Indian Institute of Technology Delhi. He was born on 23 June 1991 in a small town Diphu, Assam, India. He received his bachelor's degree from Gauhati University. Received his master's degree from NIT Silchar in 2017. He joined IIT Delhi in 2017 and his research work includes Water Flow Velocity Driven Modified Savonius Hydrokinetic Turbine.

Paruchuri M.V. Subbarao is a Professor in Mechanical Engineering Department Indian Institute of Technology Delhi. He received PhD degree from IIT Kanpur in 1994. His research interest includes computational and experimental micro fluid mechanics, computational study of high-speed gas dynamics, turbulent flow fluid mechanics and heat transfer. He is author 4 book and of more than 100 articles. He is currently Ray W. Herrick chair professor in Mechanical Engineering Department.